



ELSEVIER

## Physical metallurgy and magnetic behavior of Cd-stabilized b.c.c. $\beta$ -Gd alloys

J. Tang<sup>1</sup>, K.A. Gschneidner, Jr.\*

Ames Laboratory and Department of Materials Science and Engineering, Iowa State University, Ames, IA 50011-3020, USA

Received 4 May 1995; in final form 28 July 1995

### Abstract

The metallurgical and magnetic properties of Cd-stabilized b.c.c.  $\beta$ -Gd alloys were studied. The b.c.c.  $\beta$ -Gd phase could be retained at room temperature by alloying with Cd and liquid quenching. Single-phase alloys were obtained for Cd concentrations from 15 to 19 at.% Cd. Experimental data from these alloys were used to predict the physical properties of the pure b.c.c. Gd, such as the lattice parameter and the Curie temperature. Differential thermal analysis of the Gd–Cd alloys revealed a two-step revision process on heating in which the b.c.c. alloy first transformed into an intermediate h.c.p. phase and then completely transformed to the equilibrium  $\alpha$ -Gd + CdGd phases. The Gd–Cd alloys exhibit a Gabay–Toulouse-type spin glass transition from a ferromagnetic state into a spin glass + ferromagnetic mixed state about 30 K. The occurrence of spin glass behavior at 81–85 at.% Gd is unique in that this is the highest concentration of a magnetic ion observed in a crystalline, metallic spin glass system.

**Keywords:** Physical metallurgy; Magnetic properties; Gd–Cd alloys

### 1. Introduction

Most of the rare earth metals have a close-packed crystal structure (f.c.c., h.c.p or d.h.c.p.) at room temperature and a b.c.c. structure at high temperature [1]. While the physical properties, e.g. magnetic behavior, of the room temperature phases of rare earth metals have been studied extensively, little is known about the properties of the high temperature b.c.c. phase. This is because the diffusionless transformation from the b.c.c. phase to close-packed phase happens so fast that it is impossible to retain the pure b.c.c. rare earth metal at room temperature by ordinary quenching techniques. It was first demonstrated, however, by Gibson and Carlson that the b.c.c. phase of yttrium could be retained at room temperature by alloying with Mg and water quenching [2]. Miller and Daane [3] used this method and retained the high temperature b.c.c. phase for the heavy lanthanides in an attempt to confirm the existence of a b.c.c. high

temperature allotrope in pure Gd, Tb, Dy, Ho, Er, Tm and Lu. Herchenroeder et al. were successful in stabilizing b.c.c.  $\gamma$ La using the same quenching method [4]. Furthermore, Herchenroeder and Gschneidner showed that Cd is the only other element that is as effective as Mg in stabilizing the b.c.c. structure [5].

Herchenroeder et al. studied the physical metallurgy [6] and magnetic behavior [7] of Mg-stabilized b.c.c.  $\beta$ -Gd and  $\beta$ -Dy. In the case of Gd, a single-phase alloy could be retained in a window around the eutectoid composition from 23.6 at.% Mg to 29 at.% Mg, where the eutectoid composition is about 26 at.% Mg [8]. These b.c.c. Gd–Mg alloys order ferromagnetically (60–75 K) on cooling before undergoing a Gabay–Toulouse-type spin glass transition (40–50 K) into a mixed ferromagnetic plus spin glass state. One of their most interesting discoveries is that the metastable Gd–Mg alloys have the highest concentration of a magnetic atom among the known metallic spin glasses (more than 70 at.% Gd).

The purpose of this study is to continue the investigation on b.c.c. Gd alloys by expanding the study to the Gd–Cd system. The basis of this study rests on several observations and suppositions based on exten-

\* Corresponding author.

<sup>1</sup> Present address: Department of Physics, University of New Orleans, Lakefront, New Orleans, LA 70148, USA.

sions of the following facts. (1) Cd has been proven to be an effective stabilizer (similar to Mg) of the b.c.c. phase in the case of La [5], and, therefore, there is a good chance that b.c.c. Gd phase can be retained at room temperature by alloying with Cd. (2) The Gd–Cd phase diagram is known [9]. (3) The eutectoid composition of b.c.c.  $\beta$ -Gd is about 16 at.% Cd, which suggests that the best chances of obtaining metastable b.c.c. alloys would be near this composition [6]. This composition is significantly lower than that in Gd–Mg system, where the b.c.c. structure was retained from 23.6 at.% Mg to 29 at.% Mg. This provides a great opportunity to study metastable b.c.c. alloys even richer in Gd (above 80 at.% Gd) than for the Mg-stabilized b.c.c. Gd alloys, especially the spin glass behavior over this composition range. (4) By combining the data of both Gd–Mg and Gd–Cd systems, we hope to obtain better extrapolated information for pure b.c.c. Gd.

## 2. Experimental measurements and results

### 2.1. Sample preparation and characterization

The high purity Gd (99.8 at.% pure) used in this investigation was prepared at the Materials Preparation Center of the Ames Laboratory. Cd with a purity 99.999 at.% was purchased from Cominco Products Inc., Electronic Materials Department. Weighed amounts of Gd and Cd were sealed in a thin-walled Ta tube 50 mm long and 6 mm in diameter under an He partial pressure. Each sample (Gd + Cd) weighed about 3 g. These sealed samples were melted in a vacuum induction furnace at about 1400°C for about 20 min (the melting temperature of Gd is 1313°C [1]). In order to ensure homogeneity the crucibles were inverted and samples were remelted at about 1400°C and then cooled to room temperature.

Quenching was done as described below. The Ta crucible containing sample was sealed in a quartz tube under He partial pressure to prevent the reaction of Ta with air when heating. It was then placed in a resistance furnace and heated for a half hour at 1200°C, which is about 100°C above the liquidus temperature. This was to ensure that a homogeneous melted alloy was obtained. By quickly removing the quartz tube out of furnace and breaking it, the Ta crucible was dropped into an ice water–acetone bath. This liquid quenching technique was shown to be more effective than quenching from within the  $\beta$ -Gd region [6]. The small amount of sample and a thin-walled crucible used helped to reach the appropriate quenching speed necessary to retain the  $\beta$  phase of the Gd–Cd alloy.

Samples with compositions of 15, 16, 17 and 19 at.%

Cd, which are in the vicinity of the eutectoid composition (about 16 at.% Cd), were prepared and examined by X-rays using a rotating diffractometer and Cu K $\alpha$  radiation. X-ray diffraction analyses indicated that all samples are single phase and have the b.c.c. structure. Powder samples for the X-ray analysis were not used because the cold working required to produce the metallic alloy powder would cause the transformation from the metastable b.c.c. phase to equilibrium phases [3]. Slices of bulk sample were mechanically polished on a 600 grit paper and then on a microcloth-covered lap using a fine powder suspension of Al<sub>2</sub>O<sub>3</sub> in methanol. The polished samples were then etched with solution of 5% nitric acid in water and rinsed with methanol and acetone. Samples were spun during the X-ray experiment to reduce the effect due to preferred orientation. A typical X-ray pattern obtained from a quenched b.c.c. Gd–Cd single-phase alloy is shown in Fig. 1. As is seen, the peaks are sharp and narrow as one would expect for a well-annealed b.c.c. structure.

The lattice parameter  $a$  for each alloy was determined from X-ray data. It was noticed for all alloys that, although the  $a$  determined from the different reflections planes varied in a systematic way, there was a notable random scatter of  $a$  as  $f(\theta)$  (where  $f(\theta)$  is one of the standard extrapolation functions) such that it was difficult to obtain a meaningful extrapolated lattice parameter. Part of this may be due to compressive and tensional stresses which developed in the quenching process. This could lead to different peak widths for the different planes and thus slight line shifts (both positive and negative) which affect the various Bragg peaks differently. Therefore, as was done by Herchenroeder et al. [6], we arbitrarily chose the (211) peak to calculate the lattice parameter because it (the (211) reflection) was repeatedly the highest angle peak ( $2\theta \approx 57^\circ$ ) with a reasonably high intensity.

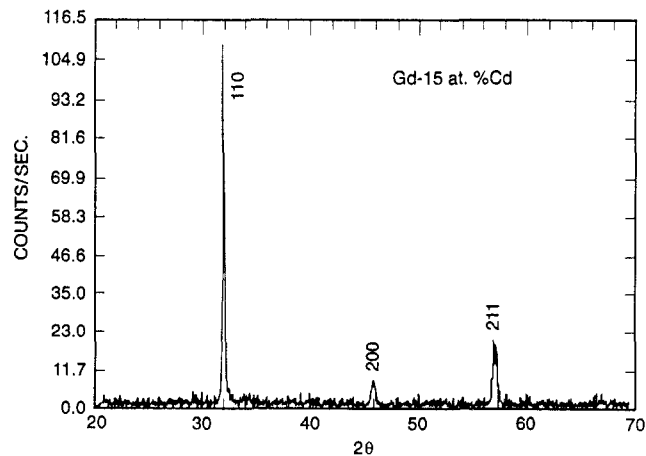


Fig. 1. X-ray diffraction pattern for quenched single-phase b.c.c. Gd-15 at.% Cd.

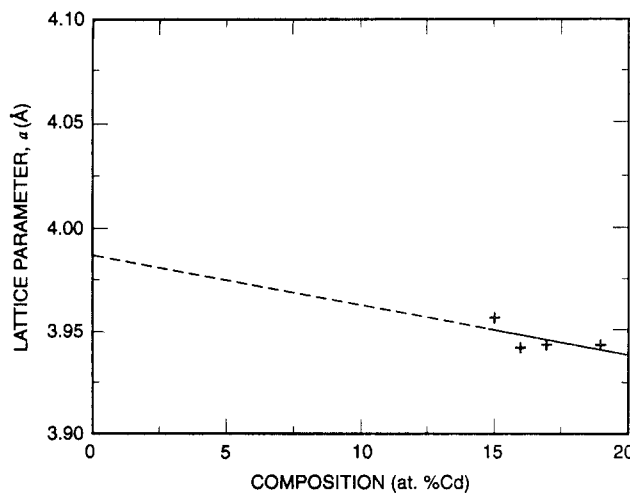


Fig. 2. Lattice parameter  $a$  vs. Cd concentration of Gd–Cd alloys.

The lattice parameters so determined were used to estimate the lattice parameter of pure b.c.c. Gd, as shown in Fig. 2 from the  $a$  vs. alloy concentration plot. A linear extrapolation to 0% Cd gives a lattice parameter of  $3.99 \pm 0.04$  Å for pure b.c.c. Gd. This value is in reasonably good agreement with the values reported earlier ( $a = 4.06$  Å, from quenching Gd–Mg b.c.c. alloy data, and  $a = 4.01$  Å, high temperature value, corrected to room temperature [6]).

The sample preparation for optical metallographic examination was carried out following a similar procedure to that used for preparing X-ray samples. All samples had basically the same kind of microstructure, which is illustrated for the Gd–16 at.% Cd alloy in Fig. 3. As can be seen, it is essentially a single-phase alloy. Two types of microstructure can be recognized: type 1 (as shown in the upper part of Fig. 3), where small grains of size about 5  $\mu\text{m}$  form a fishnet-like pattern, and type 2 (lower part of Fig. 3) which contains rather large grains (about 100  $\mu\text{m}$ ). A chemical analysis using energy-dispersive spectroscopy (EDS) revealed no apparent difference in Cd concentration between the two regions within the resolution of the EDS instrument, which is about 2 at.%. However, in the type 1 region the black-colored boundaries which separate small grains could be the traces of second phase. Magnetic measurements on these alloys supported this conclusion (see Section 2.2.1). Since the amount of the second phase is small (about 1%), X-ray and EDS methods cannot detect them. In the type 2 region, the dendritic growth from the liquid phase on quenching is evident. During the quenching the samples probably stayed in the b.c.c. single-phase region for a sufficiently long time, which allowed some annealing and homogenization to take place, and this explains why the dendritic structure was somewhat smeared out.



Fig. 3. Photomicrograph of quenched Gd–16 at.% Cd. (Magnification: 250 $\times$ .)

## 2.2. Magnetic and thermal properties

The low temperature properties of the Gd–Cd alloys were investigated by magnetic susceptibility and heat capacity measurements. Most magnetic measurements were made from 1.5 K to about 300 K using a Faraday magnetometer. A detailed description of such a magnetometer can be found in Refs. [10] and [11]. A superconducting quantum interference device magnetometer was used to examine the low field magnetic susceptibility. Low temperature (1.3 K–70 K) heat capacity measurements were carried out using an adiabatic heat pulse type calorimeter [11,12].

### 2.2.1. Magnetic susceptibility

Fig. 4 shows the magnetic moment vs. temperature of the Gd–17 at.% Cd sample which shows the common features of all of the Gd–Cd alloys studied. Data were taken from 1.5 K to about 300 K using different measuring fields from 0.5 T to 1.7 T. The system undergoes a ferromagnetic phase transition at about 85 K. As can be seen, the transition takes place over a broad temperature range. Therefore, the Curie temperature  $T_c$  was determined from an Arrott plot

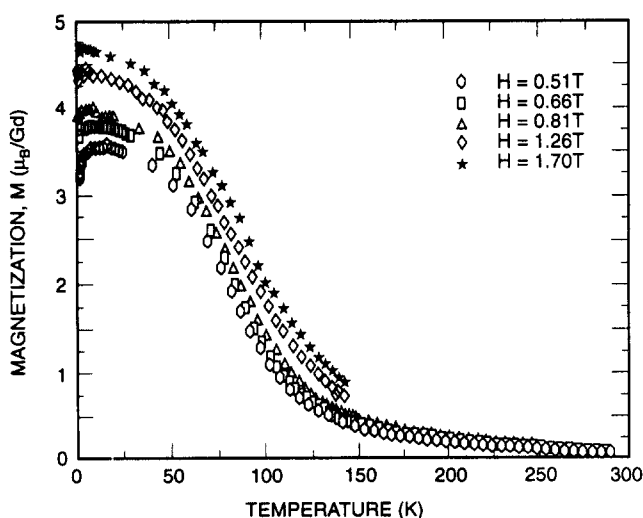


Fig. 4. Magnetic moment vs. temperature for Gd-17 at.% Cd. Data were taken from 1.5 K to about 300 K in fields of 0.51, 0.66 and 0.81 T and from 1.5 K to 140 K in fields of 1.26 and 1.70 T.

[13] for each alloy. A typical Arrott plot is shown in Fig. 5 for the Gd-17 at.% Cd alloy. The  $T_c$  values determined for these alloys are listed in Table 1.

The fact that  $T_c$  decreases with increasing Cd concentration is not surprising. Cd addition changes the average number of Gd–Gd nearest neighbors and the average distance between them, and thus weakens

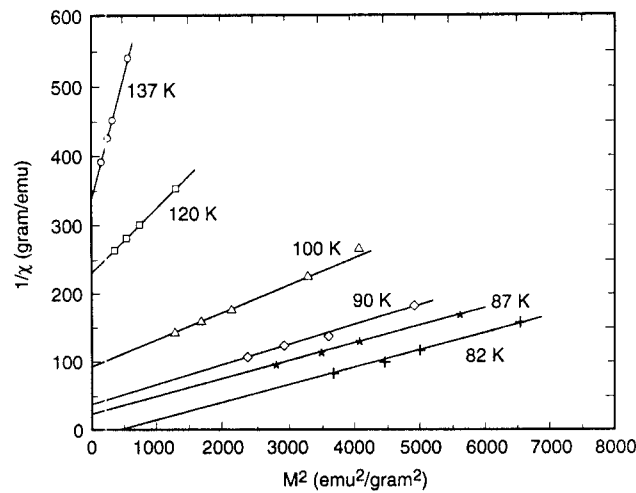


Fig. 5. Arrott plot for Gd-17 at.% Cd.

Table 1  
Magnetic transition temperatures of the metastable b.c.c. Gd–Cd alloys

Alloy	$T_c$ (K)	$T_f$ (K)
Gd-19 at.% Cd	77	36
Gd-17 at.% Cd	84	25
Gd-16 at.% Cd	85	23.5
Gd-15 at.% Cd	88	23.5

the strength of the Ruderman–Kittel–Kasuya–Yoshida interaction which is responsible for the ferromagnetic ordering in the system.

The  $T_c$  values of these alloys can be used to estimate the ordering temperature for pure b.c.c. Gd. This was done by plotting  $T_c$  as a function of Cd concentration and extrapolating the curve to 0% Cd. The extrapolated ordering temperature for b.c.c. Gd is 128.5 K. A similar extrapolation from the Gd–Mg alloys [7] gave a  $T_c$  of 133.7 K for b.c.c. Gd. Combining the two sets of data, one can conclude that the ordering temperature of pure b.c.c. Gd is  $131 \pm 3$  K. In the previous work on the Gd–Mg alloys [7], Herchenroeder and Gschneidner estimated the  $T_c$  of b.c.c. Gd to be 145 K. This value seems to be too high because these researchers relied on the three high Mg concentration alloys and did not use a least-squares fit of the data. We believe the 133.7 K value obtained from the least-squares fit of their data to be more reliable.

The magnetic moment associated with the ferromagnetic ordering is relatively small. Shown in Fig. 6 is the field dependence of the magnetization of the Gd-17 at.% Cd sample. Above  $T_c$ , the  $M$  vs.  $H$  plot exhibits a straight line behavior, indicating that the system was in a paramagnetic state. Below  $T_c$ , the moment showed no sign of saturation even in a field of 1.7 T and at a temperature of 4.2 K. The maximum measured moment per Gd atom is less than  $5\mu_B$ , which is significantly lower than the expected  $gJ$  value of Gd,  $7\mu_B$  [14]. This is due to the coexistence of strong anti-ferromagnetic interactions within the ferromagnetically ordered state as will be discussed next.

Shown in Fig. 7 is the magnetic susceptibility of the Gd-19 at.% Cd sample measured using a field of 50 G. The measurements were made under both ZFC and FC conditions. At high temperature there is hardly any difference in  $\chi$  for the ZFC and FC runs.

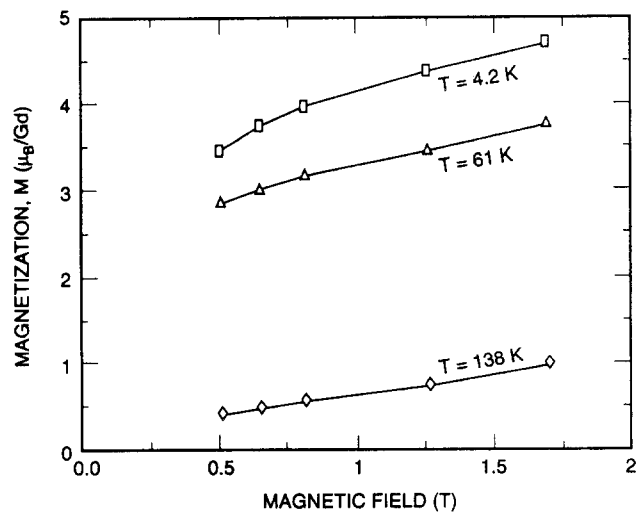


Fig. 6. Field dependence of magnetization of Gd-17 at.% Cd.

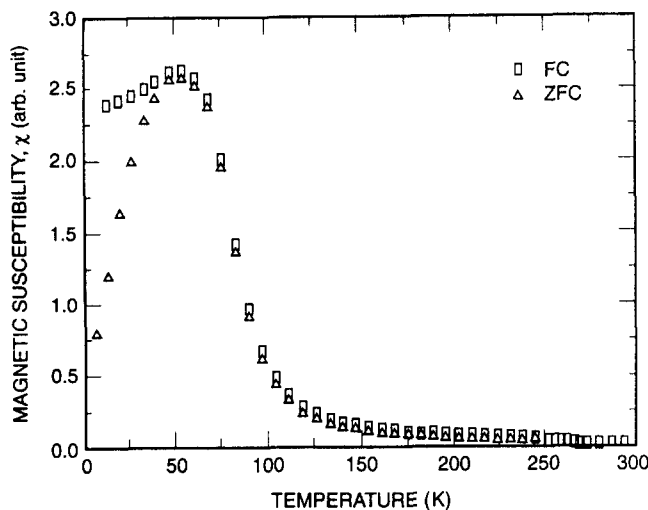


Fig. 7. Field-cooled (FC) and zero-field-cooled (ZFC) magnetic susceptibility of Gd-19 at.% Cd.

However, at low temperature (below about 50 K), there is a significant difference in the susceptibilities. In the ZFC case  $\chi$  dropped rapidly after it reached a maximum at about 55 K; in the FC case  $\chi$  is almost a constant. This is typical of spin glass behavior.

The irreversible magnetic susceptibility between ZFC and FC found in Gd-19 at.% Cd is universal among the Gd–Cd alloys suggesting that all alloys undergo a Gabay–Toulouse-type phase transition from the ferromagnetic state to the ferromagnetic + spin glass mixed state. This spin glass behavior (1) exists at high concentration of the magnetic atom (81–85 at.% Gd), which is even higher than that found in Gd–Mg alloys and (2) indicates that there are strongly competing ferromagnetic and antiferromagnetic interactions in the ferromagnetically ordered state.

The spin glass freezing temperature  $T_f$  was determined for all Gd–Cd alloys studied.  $T_f$  is defined as the intersection between a linear extrapolation of the low temperature side of  $\chi_{ZFC}$  and a horizontal line tangent to the  $\chi_{ZFC}$  maximum. The  $T_f$  values which were determined in this manner are also listed in Table 1. It is clear that  $T_f$  decreases with increasing Gd composition. It implies that, as the ferromagnetic coupling between Gd atoms becomes stronger (as a result of increasing Gd concentration), the spin glass state becomes weaker.

A small step in low field susceptibility at about 260 K (see Fig. 7) is probably due to the presence of a second phase in the samples. The most probable second phase would be either  $\alpha$ -Gd or CdGd or both as implied from the Gd–Cd phase diagram. Both of them order ferromagnetically. While  $\alpha$ -Gd has a Curie temperature just below room temperature ( $T_c = 293$  K) [14], the  $T_c$  of CdGd is reported to be 254–265 K

[15,16], which is the temperature where the step in  $\chi$  develops. Although it seems to be more likely that CdGd exists in the samples as an impurity phase because its  $T_c$  is near the step in  $\chi$ , the presence of  $\alpha$ -Gd in the samples is also possible. It was shown by Herchenroeder and Gschneidner [7] that the Curie temperature of the  $\alpha$ -Gd–Mg alloys decreases linearly with increasing Mg concentration.  $T_c$  reaches a value as low as 250 K for a concentration of 5 at.% Mg. Therefore, it is possible that the  $T_c$  of an approximately 5 at.% Cd  $\alpha$ Gd–Cd alloy is in the vicinity of 250–260 K.

The amount of CdGd ( $\alpha$ -Gd) was estimated from a magnetization  $M$  vs. applied field  $H$  plot near 200 K by extrapolating the curve to zero field and finding the intercept  $M_0$ . Since the saturation moment is  $6\mu_B$  (Gd atom) $^{-1}$  for pure CdGd [15] ( $7.0\mu_B$  for pure  $\alpha$ -Gd [14]), an  $M_0$  of  $0.062\mu_B$  (Gd atom) $^{-1}$  implies that less than 1% of the impurity phase CdGd ( $\alpha$ -Gd) is present in the alloy, which is consistent with the metallographic results; see Fig. 3.

### 2.2.2. Heat capacity

The low temperature heat capacity of the Gd-16 at.% Cd can be fitted to the equation

$$C = \gamma'T + \beta T^3 + \delta T^{3/2} \quad (1)$$

where  $\gamma'T$  is the sum of the spin glass contribution [17] and electronic contribution  $\gamma T$ ,  $\beta T^3$  the lattice heat capacity, and  $\delta T^{3/2}$  the ferromagnetic heat capacity [18]. The fitting was done by a least-squares fit method, and the constants  $\gamma'$ ,  $\beta$  and  $\delta$  were thus determined.

The coefficient  $\gamma'$  of the sum of spin glass and electronic contributions to the heat capacity is  $26 \pm 2$   $\text{mJ mol}^{-1} \text{K}^{-2}$ . To separate the two is difficult. Leung et al. [19] predicted that  $\gamma$  for ferromagnetic b.c.c. Gd is  $11.4 \text{ mJ mol}^{-1} \text{K}^{-2}$ . If this value is taken as an estimate of the real  $\gamma$  of Gd-16 at.% Cd, the linear coefficient  $\gamma' - \gamma$  of spin glass heat capacity is about  $15 \text{ mJ mol}^{-1} \text{K}^{-2}$ .

Debye temperature  $\theta_D$  was calculated from constant  $\beta$  ( $\beta = 0.68 \pm 0.05 \text{ mJ mol}^{-1} \text{K}^{-4}$ ). A  $\theta_D$  of 142 K for Gd-16 at.% Cd is slightly lower than those determined for Gd–Mg system, where  $\theta_D$  is about 170–190 K [7]. Comparing the Debye temperatures of Cd and Mg (120 K and 318 K respectively) with that of  $\alpha$ -Gd (169 K) [14,20], it is reasonable to believe that Cd additions would lower the  $\theta_D$  of b.c.c. Gd and Mg additions would increase  $\theta_D$ . (The Debye temperature also depends on the crystal structure in addition to the force constants between the atoms and their masses. Strictly speaking, the Cd addition does not necessarily lower the  $\theta_D$  of b.c.c. Gd because of its low  $\theta_D$ . However, it is true that Cd and most Cd intermetallics

are soft materials.) Based on the above assumption, the Debye temperature of pure b.c.c. Gd would be expected to lie somewhere between 140 K and 170 K.

The coefficient  $\delta$  of the magnetic contribution to the heat capacity determined from the fitting process is  $31 \pm 1 \text{ mJ mol}^{-1} \text{ K}^{-5/2}$ , which is about the same as that found in the Gd–Mg system [7].

The successful fitting of Eq. (1) to experimental data suggests that the heat capacity can be deconvoluted into lattice, ferromagnetic, spin glass and electronic heat capacities. In other words, it indicates that both the ferromagnetic state and the spin glass state exist in these Gd–Cd alloys even at the lowest temperatures, supporting the conclusion that the system is in a mixed spin glass plus ferromagnetic state below  $T_f$ .

### 2.3. Thermal stability of Gd–Cd alloys

Differential thermal analyses (DTA) were made on all of the Gd–Cd samples using a Perkin–Elmer DTA unit. Samples of 30–150 mg were used, and the heating rate varied from  $2^\circ\text{C min}^{-1}$  to  $10^\circ\text{C min}^{-1}$  in order to obtain the optimum DTA data.

Shown in Fig. 8 is the DTA curve for sample Gd–17 at.% Cd. Two small peaks are observed at  $407^\circ\text{C}$  and  $468^\circ\text{C}$ , indicating two exothermic reactions. A strong endothermic reaction can be seen at about  $740^\circ\text{C}$ , corresponding to the eutectoid transformation from low temperature phase to high temperature phase. The eutectoid temperature obtained from this study ( $738^\circ\text{C}$ ) is slightly higher than that reported earlier,  $725^\circ\text{C}$  [9].

The two exothermic reactions in this system occur at about the same temperatures where the two reversion reactions take place in Gd–Mg system [6]. It is, therefore, reasonable to assume that the b.c.c. Gd–17 at.% Cd undergoes a similar decomposition process to

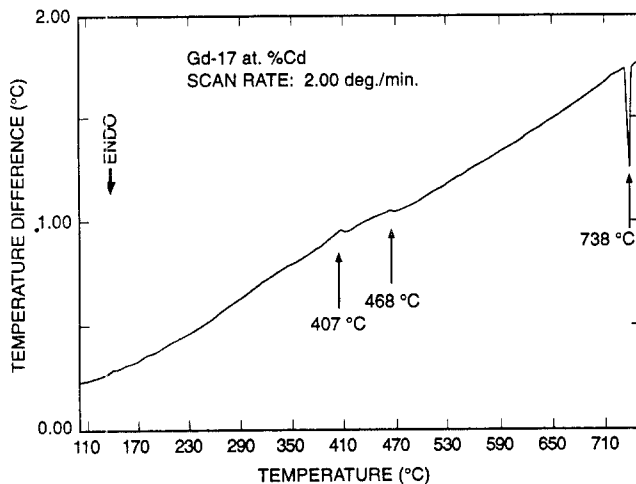


Fig. 8. DTA curve for Gd–17 at.% Cd.

that of Gd–Mg alloys, i.e. b.c.c. Gd–17 at.% Cd first transforms to an intermediate h.c.p. phase at  $407^\circ\text{C}$  and then transforms to equilibrium  $\alpha$ -Gd + CdGd phase at  $468^\circ\text{C}$ . This two-step reversion reaction has been observed in all the Gd–Cd alloys. Fig. 9 shows the reversion temperatures of the b.c.c. Gd–Cd alloys as a function of Cd concentration. The uncertainties in the transformation temperatures as discussed above are indicated by the error bars. For those points with no error bars, the uncertainties are about the same as the size of the symbol. Temperature  $T_1$  increases as the Cd concentration moves towards eutectoid composition (about 16 at.% Cd) suggesting that b.c.c. Gd–Cd alloys are more stable near the eutectoid compositions. Temperature  $T_2$  seems to be quite scattered and it is centered about  $475^\circ\text{C}$ . For comparison, the reversion temperatures of the b.c.c. Gd–Mg alloys are also shown in Fig. 9.

The following experiments were carried out to determine the stability of b.c.c. Gd–Cd alloys at lower temperatures. A piece of Gd–17 at.% Cd sample was sealed in a quartz tube under He partial pressure and heated to  $415^\circ\text{C}$  at a rate of  $15^\circ\text{C min}^{-1}$ . The sample was quickly cooled to room temperature and was examined by X-rays. One would have expected such a heat-treated sample to contain the intermediate h.c.p. phase because it was heated just above  $T_1$  ( $T_1 = 407^\circ\text{C}$ ). The X-ray pattern revealed, however, the existence of both h.c.p. and CdGd peaks, indicating that CdGd phase has already precipitated out at this temperature. Another piece cut from the same sample was heated to  $380^\circ\text{C}$  at a rate of  $20^\circ\text{C min}^{-1}$  in a similar environment. X-ray examination showed again CdGd peaks in addition to the h.c.p.  $\alpha$ -Gd + b.c.c.  $\beta$ -Gd pattern. This finding suggests that the second

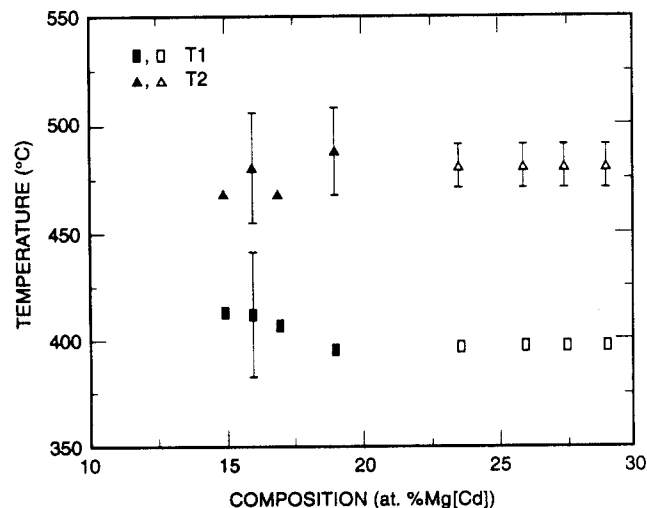


Fig. 9. The reversion temperatures of b.c.c. Gd–Mg(Cd) alloys: ■, ▲, data for the Gd–Cd alloys (this study); □, △, data for the Gd–Mg alloys [6].

reversion reaction from the intermediate h.c.p. phase to  $\alpha$ -Gd + CdGd phase can start as early as about 380°C, which is even below the first reversion temperature  $T_1$ .

The first reversion reaction took place far below  $T_1$ . It actually started at about 250°C. This was indicated by the appearance of h.c.p. peaks in the X-ray pattern of a sample which was heated to 250°C under similar conditions to those described above. No peaks from CdGd could be identified. It appears that initial transformation from b.c.c. Gd to the intermediate h.c.p. phase starts quite early but released very little energy, possibly because only local atomic rearrangements are occurring, while the release of a large amount of energy which could be detected by DTA occurs at a higher temperature  $T_1$  as more atomic movement is possible. The situation is the same in the second reversion reaction from the intermediate h.c.p. phase to the equilibrium  $\alpha$ -Gd + CdGd phase.

The metastable b.c.c. Gd phase was still evident in the X-ray pattern, after the sample was heated to 100, 250, 330 and 380°C. Its absence was first noted in the sample heated to 415°C, just above  $T_1$ . This is consistent with the above conclusion that the major portion of the transformation from b.c.c. Gd to the intermediate h.c.p. phase takes place near  $T_1$ .

### 3. Conclusions

The b.c.c.  $\beta$ -Gd was successfully retained at room temperature by alloying with Cd and quenching the liquid alloy in an ice water–acetone bath. An essentially single-phase alloy could be retained for Cd concentrations from 15 at.% Cd to 19 at.% Cd, which is in the vicinity of the eutectoid composition of (about 16 at.% Cd)  $\beta$ -Gd in the Gd–Cd system. The lattice constants obtained for these alloys were used to determine the lattice constant of pure b.c.c. Gd by extrapolation to 0 at.% Cd. Good agreement between this extrapolated value and that obtained from Gd–Mg alloys by using the same method supports the validity of such an extrapolation method. The thermal stability of these metastable b.c.c. Gd–Cd alloys was examined by DTA. Similar to Gd–Mg alloys, the Gd–Cd alloys underwent a two-step reversion process on heating in which the b.c.c. alloy first transformed into an intermediate distorted h.c.p. phase and then transformed completely to the equilibrium  $\alpha$ -Gd + CdGd phases. The initial transformation of the first reversion took place as early as 250°C, which is at a lower temperature than that found in Gd–Mg system (300°C). Consequently, the b.c.c. phase is less stable in the Gd–Cd system than in the Gd–Mg system. This is not unexpected if one realizes the fact that the metallic radius of Gd is closer to that of Mg than to Cd. A

relatively large size difference between Gd and Cd atoms makes b.c.c. Gd–Cd alloys less stable.

The magnetic behavior of these Gd–Cd alloys is most interesting. They undergo a ferromagnetic phase transition at 77–88 K and then enter a spin glass + ferromagnetic mixed state at 23–36 K. This Gabay–Toulouse-type spin glass transition is clearly seen as one compares the susceptibilities of a sample cooled in zero field and with one cooled in an applied field. That spin glass behavior exists over a high Gd concentration range (81–85 at.% Gd), which is by far the highest concentration of magnetic atom known to exhibit spin glass behavior in a crystalline metallic system, indicates a strong competition between ferromagnetic and antiferromagnetic interactions within the ferromagnetically ordered state. Low temperature heat capacity can be deconvoluted into the lattice, ferromagnetic, spin glass and electronic contributions. The appearance of both ferromagnetic and spin glass contributions to the heat capacity supports the conclusion that the final state is a mixed spin glass plus ferromagnetic state below  $T_f$ .

The ferromagnetic ordering temperature  $T_c$  was obtained for each alloy, and  $T_c$  for pure b.c.c. Gd was determined using an extrapolation method. Combining the data from the Gd–Cd and Gd–Mg alloy systems, a value of 131 K is obtained for  $T_c$  for pure b.c.c. Gd metal.

Knowing the values of  $T_c$  and  $T_f$  for Gd–Cd alloys, the magnetic phase diagram determined from the Gd–Mg system can be extended to high Gd concentration. Assuming that the magnetic property depends only on the Gd concentration and is independent of the alloying element, Cd or Mg, the high Gd concentration part obtained in this study is added to the magnetic

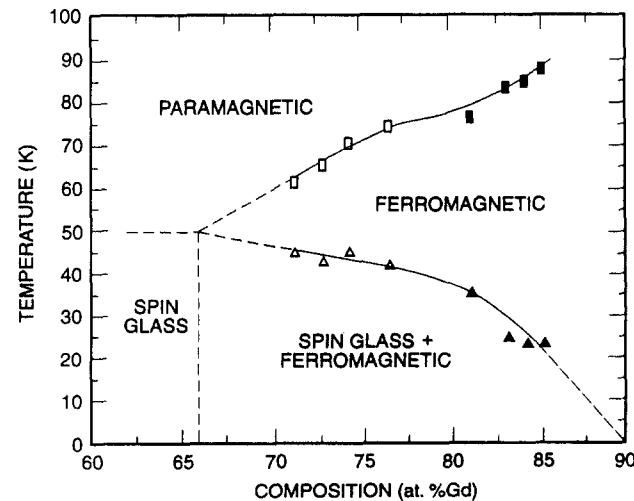


Fig. 10. Magnetic phase diagram of b.c.c. Gd–Mg(Cd) alloy: ■, ▲, data for the Gd–Cd alloys (this study); □, △, data are for the Gd–Mg alloys [6].

phase diagram of Gd–Mg system reported earlier by Herchenroeder and Gschneidner [7] and is shown in Fig. 10. As the Gd concentration increases,  $T_c$  increases and is approaching the Curie temperature of pure b.c.c. Gd. On the contrary,  $T_f$  decreases with increasing Gd concentration and tends to become zero at a concentration of about 90 at.% Gd which is expected.

### Acknowledgments

The authors wish to thank Dr. V.K. Pecharsky and J.O. Moorman for their helpful discussions and assistance in carrying out some of the experiments. This work was supported by the US Department of Energy, Office of Basic Energy Science, under Contract W-7405-ENG-82.

### References

- [1] B.J. Beaudry and K.A. Gschneidner, Jr., in K.A. Gschneidner, Jr. and L. Eyring (eds.), *Handbook on the Physics and Chemistry of Rare Earths*, Vol. 1, North-Holland, Amsterdam, 1978, p. 173.
- [2] K.A. Gschneidner, Jr. and A.H. Daane, in K.A. Gschneidner, Jr. and L. Eyring (eds.), *Handbook on the Physics and Chemistry of Rare Earths*, Vol. 11, Elsevier, Amsterdam, 1988, p. 409.
- [3] E.G. Gibson and O.N. Carlson, *Trans. Am. Soc. Met.*, 52 (1960) 1084.
- [4] A.E. Miller and A.H. Daane, *Trans. Metall. Soc. AIME*, 280 (1964) 568.
- [5] J.W. Herchenroeder, P. Manfrinetti and K.A. Gschneidner, Jr., *Physica B*, 135 (1985) 445.
- [6] J.W. Herchenroeder and K.A. Gschneidner, Jr., *Bull. Alloy Phase Diagr.*, 9 (1988) 2.
- [7] J.W. Herchenroeder and K.A. Gschneidner, Jr., *Phys. Rev. B*, 39 (1989) 11850.
- [8] P. Manfrinetti and K.A. Gschneidner, Jr., *J. Less-Common Met.*, 123 (1986) 267.
- [9] G. Bruzzone, M.L. Fornasini and F. Merlo, *J. Less-Common Met.*, 25 (1971) 295.
- [10] R.J. Stierman, K.A. Gschneidner, Jr., T.-W.E. Tsang, F.A. Schmidt, P. Klavins, R.N. Shelton, J. Queen and S. Legvold, *J. Magn. Magn. Mater.*, 36 (1983) 249.
- [11] J. Tang, *Ph.D. Thesis*, Iowa State University, 1989.
- [12] K. Ikeda, K.A. Gschneidner, Jr., B.J. Beaudry and U. Atzmony, *Phys. Rev. B*, 25 (1982) 4604.
- [13] J. Crangle, *The Magnetic Properties of Solids*, Arnold, London, 1977, p. 166.
- [14] K.A. Gschneidner, Jr., in R. Weast (ed.), *CRC Handbook of Chemistry and Physics*, CRC press, Boca Raton, FL, 69th edn., 1988, p. B-208.
- [15] G.T. Alfieri, E. Banks, K. Kanematsu and T. Ohoyama, *J. Phys. Soc. Jpn.*, 23 (1967) 507.
- [16] K.H.J. Buschow, *J. Chem. Phys.*, 61 (1974) 4666.
- [17] L.E. Wenger and P.H. Keesom, *Phys. Rev. B*, 13 (1976) 4053.
- [18] E. Gopal, *Specific Heats at Low Temperatures*, Plenum, New York, 1966.
- [19] T.C. Leung, X.W. Wang and B.N. Harmon, *Physica B*, 149 (1988) 131.
- [20] N.W. Ashcroft and N.D. Mermin, *Solid State Physics*, Holt, Rinehart and Winston, New York, 1976, p. 461.